

Paper ID MD 13

STUDY OF GROOVES PROFILE AND PERFORMANCE OF HYDRODYNAMIC BEARING

Mr. S S Shirbhate

Department of Mechanical Engineering, ICEM,Pune,India
siddheshwar.shirbhate@indiraicem.ac.in

Mr. Ashwin S Dharme

Department of Mechanical Engineering, ICEM,Pune,India
ashwin.dharme@indiraicem.ac.in

Mr. Hanumant Jagdale

Department of Mechanical Engineering, ICEM,Pune,India hanumant.jagdale@indiraicem.ac.in

Abstract

A growing interest is given to the textured hydrodynamic lubricated contacts. The use of textured surfaces with different shapes of micro cavities (textures) and at different locations of the texture zone can be an effective approach to improve the performance of bearings. The present study examines the texture location influence on the hydrodynamic journal bearing performance. A numerical modeling is used to analyse the cylindrical texture shape effect on the characteristics of a hydrodynamic journal bearing. The theoretical results show that the most important characteristics can be improved through an appropriate arrangement of the textured area on the contact surface. Tribology is a science that covers the study of friction, wear, lubrication, and contact mechanics. It permits to understand the surface interactions and to propose solutions for essential problems. The expanding range of tribological applications, habitually from industrial machinery to microscopic applications recently, has revived the importance and interest in this field. The hydrodynamic bearings are frequently used in wide range of applications and mechanisms since long.

I. Introduction

Tribology is a science that covers the study of friction, wear, lubrication, and contact mechanics. It permits to understand the surface interactions and to Propose Solutions For Essential Problems. The Expanding Range Of Tribological Applications, habitually from industrial machinery to microscopic applications recently, has revived the importance and interest in this field. The hydrodynamic bearings are frequently used in wide range of applications and mechanisms since long. Many works were dedicated to the study of the random influence roughness on the hydrodynamic journal bearing performance; the conclusion was that the roughness influences the bearing performance. the random roughness in hydrodynamic bearings may be introduced due to the presence of dust, additives in the lubricant and wear while the roughness may be random or deterministic nature. the deterministic roughness that is known as surface texture was introduced deliberately on the bearings with the help of micro fabrication techniques. surface texturing is claiming progressively more attention and is expected to be an important component in future bearing structure design as demonstrated by the authors . by means of this new technology (laser surface texturing chemical etching novel dressing technique, etc.), it is now possible to produce controlled microgeometries (textures) on journal bearing surfaces to improve the overall tribological performance including the friction reduction, the reliability improvement, the severity conditions increase, and the energy consumption lowering. tonder pointed out that by introducing a series of dimples or roughness at inlet of a sliding surface we can generate extra pressure and thus support higher load, this has also been confirmed by cupillard et al. kovalchenko et al. showed that laser texturing expanded the contact parameters in terms of load and speed for hydrodynamic lubrication. siripuram and stephens presents a numerical study of micro asperities effects with different shapes in sliding surface lubrication when hydrodynamic films are found. the minimum coefficient of friction for all shapes is found to occur at an asperity area fraction

of 0.2 for positive asperities and 0.7 for negative asperities. Some other and recent studies have established that the surface texture geometry such as texture depth, width, number of textures, and location of textures influence the bearing performance. In others studies Navier–Stokes equations have been solved for the flow between two parallel surfaces, one smooth and one having a single surface pocket. They showed that the pressure generating effect of surface texture in full film operation might result from convective inertia. Piezo-viscosity may play a role in heavily loaded lubricated contacts. Thus, in local converging regions the pressure rise may be larger than the pressure drop in diverging regions. Arghir et al. have shown that Navier–Stokes equations are inadequate to predict pressure build-up with the presence of macro roughness as inertia effects can be more important. This finding was confirmed later by Sahlin et al. also presented a study on the geometry optimization. According to De Kraker et al. , the use of a Reynolds equation to study the effects of texture will be valid if dimple depth is greater than minimum film thickness of the lubricant in the fluid film lubrication. Cupillard et al. have found that the mechanism of pressure build-up in a convergent gap between two sliding surfaces due to texture is similar to that obtained with convergence ratio variation for smooth surfaces. The same author found that there is an optimal texture depth, greater than the critical depth, which gives the maximum load carrying capacity. Above this depth, a global recirculation zone occurs in each dimple, leading to a loss in the load carrying capacity. In non-cavitated hydrodynamic contacts where Reynolds assumptions hold true, full texturing has a negative impact on both hydrodynamic lift and viscous friction. The positive texture effects observed in fully textured parallel sliders are explained by two theories. The first one considers the cavitation phenomena as the source of these positive effects. Accordingly, the presence of dimples creates an alternation of converging and diverging film regions, in which the pressure varies between a positive value in the lubricated regions and the vaporization pressure in the cavitated regions. Consequently, an overall positive resultant is obtained . A second theory suggests that the load capacity generated in fully textured parallel sliders is caused by inertia effects (convective inertia) . It was recently shown that this theory is inaccurate and that inertia effects have, in general, a negative influence over the hydrodynamic performance . Consequently, cavitation emerges as the main mechanism leading TO THE OBSERVED INCREASED LIFT AND REDUCED FRICTION IN FULLY

TEXTURED PARALLEL SLIDERS.

Full texture is unusable to generate hydrodynamic lift in parallel sliders, except when the dimple is replaced at the slider inlet (the generated lift is minimal). In convergent plane-inclined sliders, full texturing has negative effects.

In partially textured parallel sliders, the positive texture effects is due to the cavitation mechanism, the inlet flow is increasing and the development of full lubrication at some distance from the principal edge is allowed. But in convergent sliders, cavitation has minimal influence (affecting a small portion of the contact).

In parallel sliders, starting partial texturing at the inlet generates significant hydrodynamic lift. In plane-inclined sliders with low global film convergence, partial texturing provides soft performance improvements. In highly convergent sliders, texturing has minimal effects.

1.1 Types Of Grooves Profile

The present paper starts from the standpoint that it is unrealistic to make a direct analysis of a real problem that can possess more than thousands of macro-roughness. The purpose is then to investigate the flow in single cells of periodical macro-roughness patterns and to extract conclusions useful for lubrication's framework. The work is carried out by numerically integrating the full system of Navier Stokes equations for a laminar, incompressible and isothermal flow in macro-roughness cells. The macro-roughness is located on one of the walls while the opposite one has a parallel relative velocity. The walls are parallel and cyclic conditions are imposed on the boundaries. If the roughness would be absent a simple Couette flow is to be found with an overall constant pressure field. The

flow field induced by the presence of the macro-roughness and by the closely interacting walls possesses some interesting characteristics determined by the presence of inertia forces. The most important is the generation of a net lift force on the moving wall. This effect is further discussed from the standpoint of its possible impact on lubrication theory.

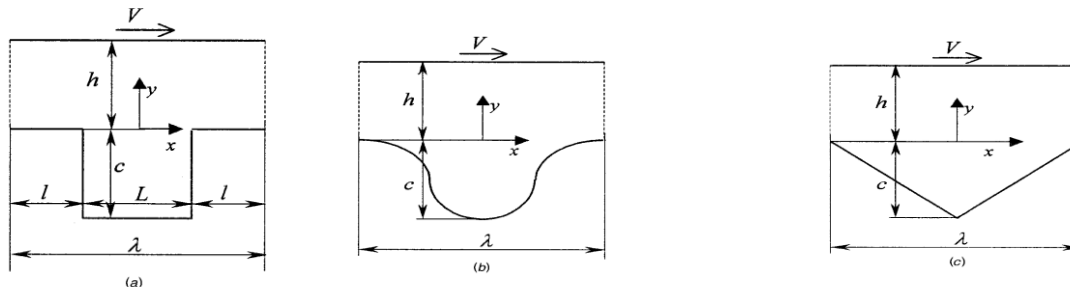


Fig. 1 Geometry of the two-dimensional macro roughness: .a.rectangular; .b. sinusoidal; and .c. triangular

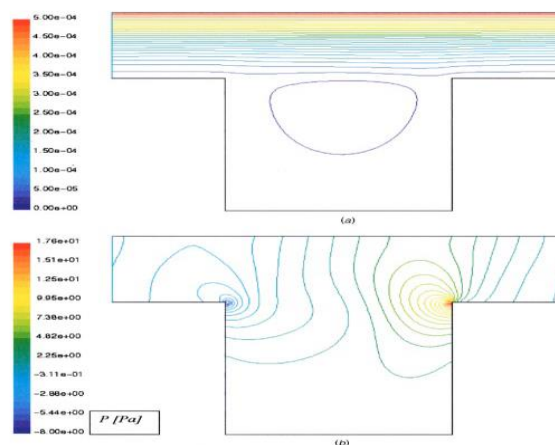


Fig. 2 .a,b. Streamlines and pressure isolines for a rectangular macro roughness

1.2 Numerical Analysis

Three types of two dimensional macro-roughness patterns, namely rectangular, sinusoidal and triangular are analysed. They represent the main part of the analysis and can be considered to stem, for example, from a striated surface. Three dimensional calculations are performed only for a cubic and for a cylindrical roughness pattern and they are aimed to validate the effects enlightened by the two dimensional analysis. All calculations are made using a finite volume code which employs the SIMPL Algorithm for integrating the Navier-Stokes equations. A structured finite volume grid employing rectangles or bricks is used for discretizing the domain.

1.3 Rectangular Two-Dimensional Macro-Roughness

The cell of a rectangular macro-roughness pattern is presented on Fig.1~a!. The film and the roughness are of equal length, $l = 5L/2$, so the pattern belongs to the Stokes kind of roughness. The upper wall translates with velocity V from left to right on all the following figures. No-slip boundary conditions are imposed on the upper and on the lower wall and cyclic boundary conditions are imposed on the left and on the right boundaries. Cyclic boundary conditions indicate that full periodicity in terms of field values and fluxes is ensured. A parametric study is performed by considering three c/l ratios, namely 0.25, 0.5, and 1. The ratio $h/c = 0.5$ is kept constant in the present examples. Four Reynolds numbers are considered, namely $Re_h = 0.5, 1, 10, 100$. The average film height used for defining the Reynolds number is $h_0 = 5h/2$. All the present reported results have been obtained after two successive grid refinements that multiplied by four at each step the original number of control volumes. For all reported results the asymptotic range was attained and the GCI is inferior to 1 percent. This special care was intended to eliminate the uncertainty introduced by some possible numerical diffusion. A zero pressure reference cell was considered on the

upper wall at the right end section. This discussion applies to all cases treated in the present work. Figures 2~a,b! present the streamlines and the pressure field . It can be seen that the streamlines present the expected pattern with a recirculation zone located in the cavity Figure 2~b! shows that pressure first diminishes at the left corner of the macro-roughness then increases when encountering the right corner. The pressure decrease and increase corresponds to an enlargement and to a diminishing transversal flow section. It can be observed that the constant pressure lines are not symmetrical about a point located at $y=50$ on the vertical midsection. The pressure rise is more important than the drop. Following this remark pressure variations on the upper wall are presented in Fig. 3 for different Reynolds numbers. The pressure first decreases due to the channel height enlargement then increases under the influence of the roughness right corner. For very small Reynolds numbers, when viscous effects are largely dominant and the approximation of the Stokes flow regime is acceptable the pressure distribution is anti symmetrical about the point located at $x=50$ and $y=50$. With the augmentation of the Reynolds number and the increased importance of inertia forces the pressure distribution becomes asymmetric, namely, the pressure rise close to the right roughness corner being more important than the pressure drop. The same observations hold for the pressure distribution along the line of $y=50$ presented in Fig. 4. The distribution is anti symmetrical about the $x=50$ and $y=50$ point for Reynolds number corresponding to creeping flows and then becomes asymmetric under the influence of the right corner which diffuses upstream in the flow. If one integrates the pressure distribution along the upper wall for very small Reynolds numbers one obtains a zero net force due to the anti symmetry of the pressure field. With increasing Reynolds number this force becomes nonzero and positive. It then means that under the increasing influence of inertia forces a lift force will be generated between the two walls. It is an effect which is exclusively due to the presence of the macro-roughness and combined with an inertia flow regime. If the macro-roughness would be absent the walls would be simply parallel and a pure Couette flow without any pressure generation would have been obtained for any Reynolds number. It then means that the simple presence of the macro-roughness and of the inertia flow regime can generate a lifting force between otherwise two parallel walls. The statement that the lift force is produced by inertia effects is also verified by varying the length occupied by the macro roughness. Figure 5 presents the pressure distributions on the upper wall for three different cases obtained by considering c/l the previous reference case! and 1, and by keeping

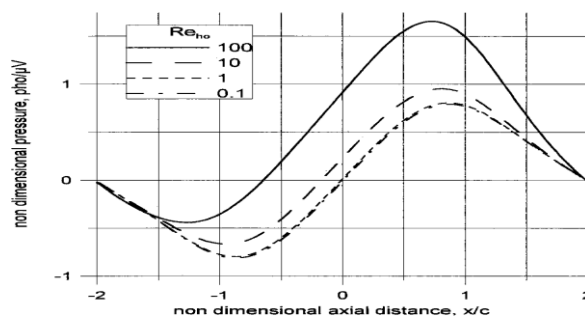


Fig. 3 Pressure distribution on the flat moving wall of the reference rectangular macro roughness

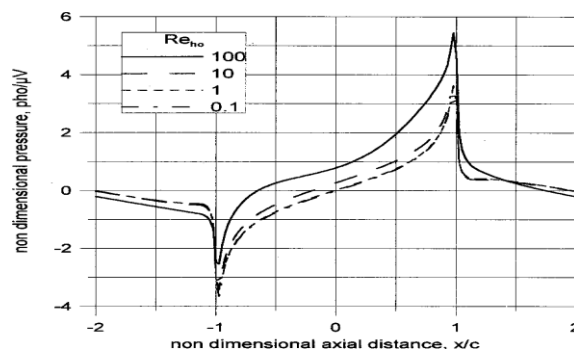


Fig. 4 Pressure distribution along the line of $y=50$ of the reference rectangular macro roughness

1.4 Sinusoidal Two-Dimensional Macro-Roughness

The lower wall now possesses a sinusoidal macro-roughness Fig. 1b. The distance c is now taken as the peak to bottom height and the calculations are made for a geometry similar to the one used for the rectangular macro-roughness, i.e., $c/150.5$ and $h/c50.5$. Figures 6~a! and 6~b! present the streamlines and the pressure. The same characteristic as for the previous type of macro-roughness are found. The streamlines present a recirculation zone located inside the cavity and slightly oriented towards the downstream part. The pressure first diminishes with the enlargement of the flow passage then increases towards the downstream zone. For the indicated Reynolds number, the pressure rise is more important than the pressure drop. This finding can again be identified as an inertia effect when analysing the pressure distribution on the upper wall for different Reynolds numbers. As shown in Fig. 7 for very low Reynolds numbers the pressure distribution is ant symmetric about $y50$ and with increasing Reynolds numbers the positive pressures progressively overweigh the negative ones. Figure 8 shows the pressure distributions on the upper wall for two different sinusoidal macro roughness the rectangular macro-roughness type, the geometry influences the form of the pressure distribution and the magnitude of the net lift effect. Strong similarities with the results reported by Sood and Elrod in can be further underlined. Thus Sood and Elrod analysed the effect of inertia forces for the flow between two infinitely long eccentric cylinders. Their calculations were made for a relative eccentricity1 of 0.5 and the value of the cantered radial clearance divided by the inner cylinder radius was 1. When developing the surfaces of the inner rotating infinitely long cylinder, the resulting geometry has, in a first approach, a sinusoidal distribution of the clearance. It can be then cast in terms of the presently employed parametric description of the sinusoidal macro-roughness. So the reference geometry analysed by Sod and Elrod is described by $c/150.16$ and $h/c50.5$. Their employed Reynolds number calculated with the linear velocity of the inner rotating cylinder and based on the equivalent of the $h0$ height was 37.2. In order to enlighten the effect of the inertia forces, So and Elrod's presented two series of calculation for the same Reynolds number, one using the Stokes system of equations the other one using the full Navier Stokes mathematical model. Pressures on the inner rotating cylinder resulting from a Stokes analysis and presented on Fig. 8 of their work show a perfect ant symmetric distribution about the minimum or the maximum clearance section. This finding is in perfect agreement with the results presently obtained for Re_{h0} and given in Fig. 7.

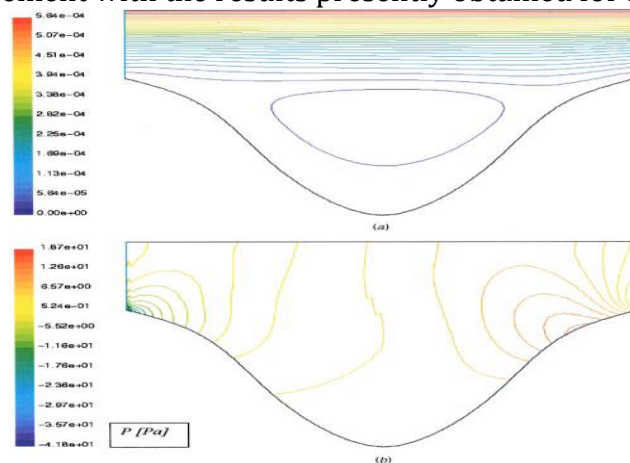


Fig. 5 .a,b. Streamlines and pressure isolines for a sinusoidal macro roughness

1.5 Triangular Sawtooth.Two-Dimensional Macro-Roughness

A triangular sawtooth! macro-roughness pattern was also analyzed. The distances and the geometric parameters are defined in the same way as for the sinusoidal macro-roughness ~Fig. 1~c!!. Figures 9~a! and 9~b! present the streamlines and the pressure field. Pressures distribution on the upper wall are presented in Figures 10 and 11. The results are very similar with the ones obtained for the sinusoidal macro-roughness. This was to be expected because these two macro-roughness are in fact very close from geometrical standpoint.

1.1.5.1 Three Dimensional Macro-Roughness

Three dimensional macro-roughness calculations were made only for the counterpart of the rectangular two-dimensional reference geometry and for $Re_h 0 5100$. They were not performed in the same systematic manner as for two-dimensional macro-roughness because the intent was only to verify the formerly underlined effects. Two three dimensional geometries can be developed from the basic two dimensional one and are shown in Fig. 14. The first consists of a parallelepiped macro-roughness having the same dimensions as the two-dimensional reference geometry in section planes containing the velocity of the moving wall and normal to it. No slip conditions are imposed on walls and cyclic boundary conditions are considered on planes normal and parallel to the velocity of the moving wall. This way the geometry simulates a single cell extracted from a pattern of three-dimensional macro-roughness aligned with the velocity of the moving wall. The second three-dimensional geometry consists of a cylindrical macro-roughness obtained by rotating the reference two-dimensional roughness around its symmetry axis. As for the first three-dimensional geometry, planes normal and parallel to the velocity of the moving wall carry cyclic boundary conditions. it can be seen that the pressure distributions of the three-dimensional geometries are very similar and follow closely the two-dimensional variation. The pressure rise produced by the downstream corner is again larger than the pressure drop due to the upstream corner and if integrating the pressure variation a lift effect is present. The lift effect is this time somewhat smaller than for the two-dimensional case. This result can be explained if one considers the problem of the drag of an infinite cylinder compared with a sphere of the same diameter in a parallel no viscous flow. The infinite cylinder represents a two-dimensional problem and its drag is higher than the one of the corresponding sphere the three-dimensional problem! because for the same three-dimensional geometry the flow has more freedom to contour the obstacle.

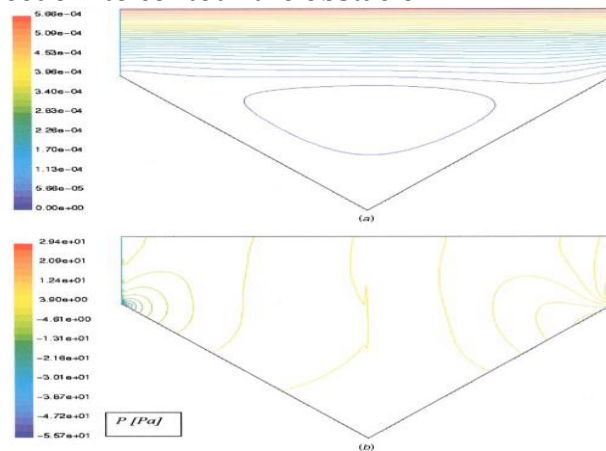


Fig. 6 .a,b. Streamlines and pressure isolines for a triangular macro roughness

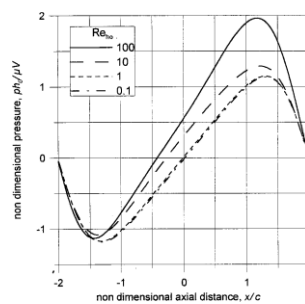


Fig. 10 Pressure distribution on the flat moving wall of the triangular macro roughness

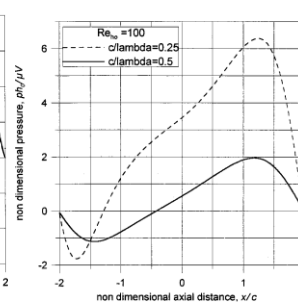


Fig. 11 Pressure distribution on the flat moving wall of different reference triangular macro roughness .

1. Conclusion

- An introduction of micro-groove on one of the surfaces affect the flow and pressure pattern.
- This gives a net pressure build-up and a load carrying capacity of the film.
- Load carrying capacity increase with Reynolds number and groove width w .
- The friction force decreases with increasing values of groove depth d and w .

2. References

1. Mihai Arghire, Nicolas Roucou Mathieu Helene Jean Frene, Theoretical Analysis of the Incompressible Laminar Flow in a Macro-Roughness Cell 2003
2. Schlichting, H., 1979, Boundary Layer Theory, McGraw-Hill, Inc.
3. Dowson, D., Taylor, C. M., Godet, M., and Berthe, D., 1978, Surface Roughness Effects in Lubrication, Proceedings of the 4th Leeds-Lyon Symposium on Tribology held in September 13–19, published by Mechanical Engineering Publications Ltd.
5. Elrod, H. G., 1979, "A General Theory for Laminar Lubrication with Reynolds Roughness," ASME J. Lubr. Technol.,
6. Citron, S. J., 1962, "Slow Viscous Flow between Rotating Concentric Infinite Cylinders with Axial Roughness," ASME J. Appl. Mech.,
7. Sun, D. C., and Chen, K. K., 1977, "First Effects of Stokes Roughness on Hydrodynamic Lubrication Technology," ASME J. Lubr. Technol.,
8. Elrod, H. G., 1977, "A Review of Theories for Fluid Dynamic Effects of Roughness on Laminar Lubricating Films," Fourth Leeds-Lyon Symposium on Tribology held in September 13–19, published by Mechanical Engineering Publications Ltd.
9. Hu, J., and Leutheusser, H. J., 1997, "Micro-Inertia Effects in Laminar Thin-Film Flow Past A Sinusoidal Boundary," ASME J. Lubr. Technol.,